

# A comparative study of Young's modulus of single-walled carbon nanotube by CPMD, MD and first principle simulations

Jin-Liang Zang, Quanzi Yuan, Feng-Chao Wang, Ya-Pu Zhao \*

State Key Laboratory of Nonlinear Mechanics, Institute of Mechanics, Chinese Academy of Sciences, Beijing 100190, People's Republic of China

## ARTICLE INFO

### Article history:

Received 11 November 2008  
Received in revised form 1 April 2009  
Accepted 4 April 2009  
Available online 8 May 2009

### PACS:

31.15.-A  
31.15.-E  
31.15.xv  
62.25.-g

### Keywords:

Car–Parrinello molecular dynamics (CPMD)  
Density functional theory (DFT)  
Molecular dynamics (MD)  
Young's modulus  
Carbon nanotubes (CNTs)  
Chirality

## ABSTRACT

Carbon nanotubes (CNTs), due to their exceptional magnetic, electrical and mechanical properties, are promising candidates for several technical applications ranging from nanoelectronic devices to composites. Young's modulus holds the special status in material properties and micro/nano-electromechanical systems (MEMS/NEMS) design. The excellently regular structures of CNTs facilitate accurate simulation of CNTs' behavior by applying a variety of theoretical methods. Here, three representative numerical methods, i.e., Car–Parrinello molecular dynamics (CPMD), density functional theory (DFT) and molecular dynamics (MD), were applied to calculate Young's modulus of single-walled carbon nanotube (SWCNT) with chirality (3,3). The comparative studies showed that the most accurate result is offered by time consuming DFT simulation. MD simulation produced a less accurate result due to neglecting electronic motions. Compared to the two preceding methods the best performance, with a balance between efficiency and precision, was deduced by CPMD.

© 2009 Elsevier B.V. All rights reserved.

## 1. Introduction

After first discovery, due to their excellent physical, chemical and mechanical properties, carbon nanotubes (CNTs) [1] continue to be one of the hottest research areas more than 18 years. These properties support CNTs to be the suitable element for transistors, quantum dots, hydrogen storage devices, chemical and electromechanical sensors, field emission, etc. [2–4]. The mechanical applications of CNTs would be also the biggest large-scale application for the material. The extremely high Young's modulus and low specific weight make the CNT become the potential reinforcement in high-performance composites.

There existed significant differences among Young's moduli obtained from different theoretical methods [5–9]. Structural rigidities of CNTs were first predicted theoretically by Overney et al. [5], using an empirical Keating Hamiltonian with parameters determined from first principles. Using molecular dynamics (MD) simulations and fitting them for the elastic shell theory, Yakobson et al. [6] calculated the Poisson ratio  $\nu = 0.19$ , effective wall thickness  $h = 0.66 \text{ \AA}$ , and Young's modulus  $Y = 5.5 \text{ TPa}$ , respectively.

Empirical Brenner potentials were employed by Robertson et al. [7] to examine the energetics and elastic properties of CNTs with radii less than  $9 \text{ \AA}$ . The Young's moduli of CNTs were found to be close to that for in-plane single-crystal graphite, about  $1.06 \text{ TPa}$ . Using MD simulations with universal force field (UFF), Yao and Lardi reported Young's moduli of CNTs were about  $1 \text{ TPa}$  [8]. Qin et al. predicted that the moduli of (5,5) and (9,0) SWCNTs were around  $0.6\text{--}0.7 \text{ TPa}$ , whereas the Lennard-Jones and the TB-G2 potentials were employed [9].

As noted from the above works, the large numbers of numerical studies on CNT dynamics were based on MD simulations. In the classical MD simulations, all degrees of freedom due to the electrons are ignored, as well as quantum effects. So a more accurate description is needed, i.e., potentials between electron–electron, electron–ion as well as ion–ion interactions should be considered. In this respect, the *ab initio* density functional theory (DFT) and Car–Parrinello molecular dynamics (CPMD) [10] were used in the study. DFT calculation, which is known as time consuming and considering more details about the electrons and the ions, can give more interactions and corrections about electron–electron, electron–ion and ion–ion, which are disregarded in classical MD. Considered these corrections, the simulated Young's moduli of CNTs would be more credible. But it can only simulate the static state.

\* Corresponding author. Tel.: +86 10 8254 3932; fax: +86 10 6256 1284.  
E-mail address: [yzhao@imech.ac.cn](mailto:yzhao@imech.ac.cn) (Y.-P. Zhao).

CPMD, which combines the MD simulation with quantum mechanics, treats the electronic degrees of freedom in the framework of DFT. It makes a balance between efficiency and precision, while considering the dynamic effect. However, the dynamic processes, performing in the CPMD still restricted to small system which is a main disadvantage of CPMD. We compendiously compared the three different methods in Table 1.

In this paper, we presented Young's moduli of CNTs calculated by CPMD, classical MD and DFT. By comparing the results of different methods, calculation errors could be estimated, the advantages and disadvantages of different methods would be revealed. This work would be helpful to choose an appropriate method to simulate some other nanomaterials.

## 2. Method

CPMD is an *ab initio* molecular dynamics method which is the combination of first principles electronic structure methods with MD based on Newton's equations of motion. Grand-state electronic structures were described according to DFT within plane-wave pseudopotential framework. The use of electronic structure methods to calculate the interaction potential between atoms overcomes the main shortcomings of the otherwise highly successful pair potential approach. There have been plenty of excellent reference books on MD and DFT, and some simulation tricks can be found [11–14]. Here, some more details about CPMD which are different from the traditional classical MD and DFT will be discussed.

In CPMD, considering the parameters  $\{\psi_i\}$ ,  $\{R_l\}$ ,  $\{\alpha_v\}$  in energy function

$$E[\{\psi_i\}, \{R_l\}, \{\alpha_v\}] = \sum_i \int_{\Omega} d^3r \psi_i^*(r) [-(\hbar^2/2m)\nabla^2] \psi_i(r) + U[n(r), \{R_l\}, \{\alpha_v\}], \quad (1)$$

are supposed to be time-dependent, the Lagrangean:

$$L = \sum_i \frac{1}{2} \mu \int_{\Omega} d^3r |\dot{\psi}_i|^2 + \sum_l \frac{1}{2} M_l \dot{R}_l^2 + \sum_v \frac{1}{2} \mu_v \dot{\alpha}_v^2 - E[\{\psi_i\}, \{R_l\}, \{\alpha_v\}], \quad (2)$$

was introduced, where the  $\psi_i$  are subject to the holonomic constraints:

$$\sum_i \int_{\Omega} d^3r \psi_i^*(r, t) \psi_j(r, t) = \delta_{ij}. \quad (3)$$

In Eqs. (1) and (2),  $\psi_i$  are orbitals for electrons,  $R_l$  indicate the nuclear coordinates and  $\alpha_v$  are all the possible external constraints imposed on the system,  $\psi^*(r)$  is the complex conjugate of wavefunction  $\psi(r)$ ,  $\hbar$  is the reduced Planck constant,  $m$  is the mass of electron and  $n(r) = \sum_i |\psi_i(r)|^2$  is the electron density; the dot indicates time derivative,  $M_l$  are the physical ionic masses, and  $\mu$ ,  $\mu_v$  are arbitrary parameters of appropriate units. Then, the equations of motion can be written as

$$\mu \ddot{\psi}_i(r, t) = -\frac{\delta E}{\delta \psi_i^*(r, t)} + \sum_k \Lambda_{ik} \psi_k(r, t), \quad (4)$$

$$M_l \ddot{R}_l = -\nabla_{R_l} E, \quad (5)$$

$$\mu_v \ddot{\alpha}_v = -\left(\frac{\partial E}{\partial \alpha_v}\right), \quad (6)$$

$\Lambda_{ik}$  are Lagrange multipliers introduced in order to satisfy the constraints in Eq. (3). Then the equation of kinetic energy

$$K = \sum_i \frac{1}{2} \mu \int_{\Omega} d^3r |\dot{\psi}_i|^2 + \sum_l \frac{1}{2} M_l \dot{R}_l^2 + \sum_v \frac{1}{2} \mu_v \dot{\alpha}_v^2, \quad (7)$$

is obtained [10]. Based on the technique mentioned, CPMD extends MD beyond the usual pair-potential approximation. In addition, it also extends the application of DFT to much larger systems.

In our work, a three-dimensional (3D) periodically repeated triclinic supercell was used and the cell was large enough to avoid the interactions between the CNTs' atoms. The interactions of the ion core with the valence electrons were described by S. Goedecker (SG) norm-conserving pseudopotential given by Goedecker and his co-workers [15]. The electronic wave functions were expanded in plane-wave basis set with the energy cutoff of 80 Ry. Local density approximation (LDA) was used and the Brillouin zone was sampled at Gamma point. The CPMD source code, version 3.13.2 [16], can be downloaded with permissions free of charge for non-profit organization.

In the MD simulation, CNT was parameterized within the consistent valence force field (CVFF) developed by Hagler et al. [17]. The most commonly used functional forms are

$$E = E_{\text{pair}} + E_{\text{bond}} + E_{\text{angle}} + E_{\text{dihedral}} + E_{\text{improper}}, \quad (8)$$

where  $E_{\text{pair}}$  is van der Waals interaction which can be expressed as the best well known Lennard-Jones 12-6 function,  $E_{\text{pair}} = 4\epsilon[(\frac{\sigma}{r})^{12} - (\frac{\sigma}{r})^6]$ ,  $r < r_c$ , here  $\sigma$  is the distance at which the inter-atom potential is zero and  $\epsilon$  is the depth of the potential well,  $r$  is the distance between atoms.  $E_{\text{bond}} = K_b (r - r_0)^2$  is the interaction between pairs of bonded atoms,  $E_{\text{angle}} = K_a (\theta - \theta_0)^2$  is the interaction of valence angles in the molecule. These two equations represent the harmonic potential that gives the increase in energy as the bond length  $r$  deviates from the reference value  $r_0$ ,  $\theta$  is the bond angle and the reference value  $\theta_0$ .  $K_b$ ,  $K_a$  are the stiffnesses of the bond and the bond angle, respectively.  $E_{\text{dihedral}} = K_d [1 + d_d \cos(n_d \phi)]$ ,  $E_{\text{improper}} = K_i [1 + d_i \cos(n_i \phi)]$  describe dihedral and improper interactions between quadruplets of atoms.  $K_d$ ,  $K_i$  are often referred to as the energy barrier height of dihedral angle and the improper angle.  $d_d$ ,  $d_i$  whose value is  $-1$  or  $+1$ , just represent the direction of the angle.  $n_d$ ,  $n_i$  are the multiplicities. The parameters used for CNTs in this force field are listed in Table 2.

All MD runs were carried out by using the large-scale atomic molecular massively parallel simulator (LAMMPS) developed by Sandia National Laboratories. LAMMPS is a classical MD open-source code [18] which is distributed under the terms of the GNU Public License. More details can be obtained from <http://lammps.sandia.gov/>.

Our first principles energy calculations were performed using DFT implemented in a CASTEP package [19], based on the plane-wave pseudopotential method. This numerical technique had been

**Table 1**  
Brief comparison of three different methods.

	Merits	Drawbacks
DFT	High accuracy; more details (electronic states, charge distribution, molecule orbits)	Limited to static states of small systems; slow and expensive
MD	Available for large systems; fast and cheap	Disable in chemical reaction (bond breaking/forming); empirical potentials are used which leads to low accuracy
CPMD	Combined MD with DFT; a balance between the time consuming and precision	Limited to dynamic process of small systems

**Table 2**

Parameters used for CNTs calculation in CVFF.

Bond coefficients		Angle coefficients		Pair coefficients		Dihedral coefficients			Improper coefficients		
$K_b$	$r_0$	$K_a$	$\theta_0$	$\varepsilon$	$\sigma$	$K_d$	$d_d$	$n_d$	$K_i$	$d_i$	$n_i$
480.000	1.340	90.000	2.094	0.148	3.617	3.000	−1.000	2.000	0.370	−1.000	2.000
kcal·(mol <sup>−1</sup> Å <sup>−2</sup> )	Å	kcal mol <sup>−1</sup>	rad	kcal mol <sup>−1</sup>	Å	kcal mol <sup>−1</sup>	–	–	kcal mol <sup>−1</sup>	–	–

proved to give the correct equilibrium structure and to be accurate enough to describe the ground state properties of CNTs [20–22]. In our calculation, the exchange correlation functional was treated under the generalized gradient approximation (GGA) with Perdew–Burke–Ernzerhof (PBE) functional [23]. Ultrasoft pseudopotentials and an energy cutoff of 400 eV, representing the number of plane wave basis sets, were used for all cases. The special points sampling integration over the Brillouin zone was employed by using the Monkhorst–Pack method [24] with a grid of  $4 \times 4 \times 2$  k-point. Self-consistent field procedure was carried out with a convergence criterion of  $10^{-6}$  a.u. on energy and electron density for all single point energy calculations.

The whole structure of simulated SWCNT and the repeated unit are shown in Fig. 1. Considering the computational complexity and time consuming in CPMD and DFT, a small but typical SWCNT with chirality (3,3) was adopted into calculation. The mechanical properties of SWCNTs with other chirality would be similar to (3,3) SWCNT. There are 12 atoms in each cell and the nanotube diameter is 4.07 Å. The dashed line cell is the repeated triclinic supercell used in the simulation. In all of calculations, the wall thickness of SWCNT was assumed to be 3.4 Å.

### 3. Results and discussion

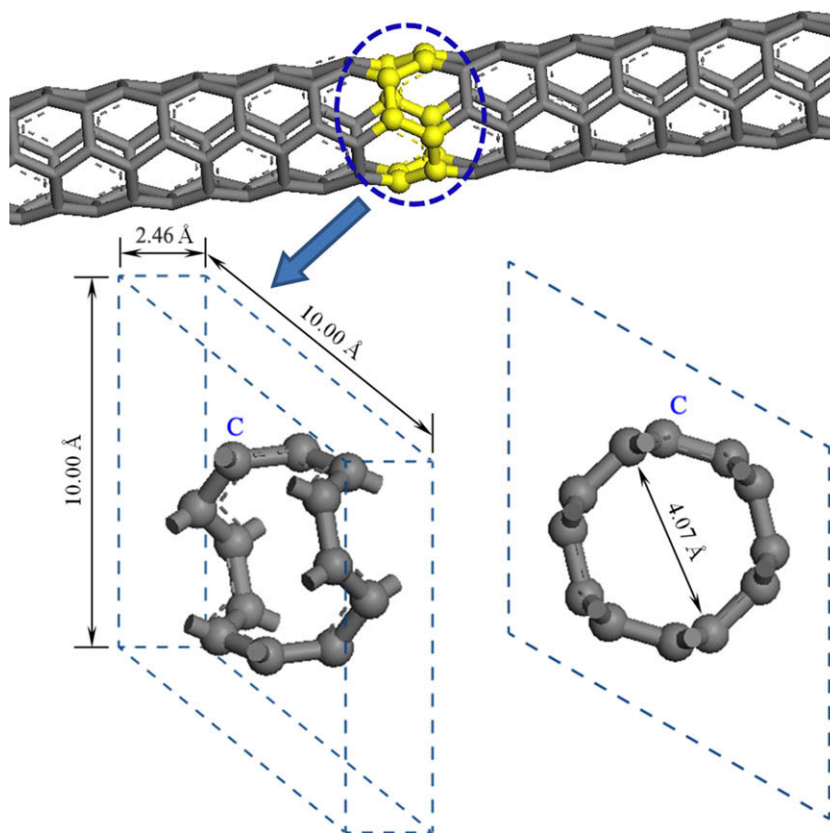
Here, different measures were adapted to deal with the results obtained from different methods. The deformation energy would be used to calculate Young's modulus in CPMD and DFT simulation. The stress–strain curve was used in dealing with MD's result.

The SWCNT was pulled step by step and the potential energy at every state was obtained. The step increase in CPMD simulation was 0.01 Å. Initial length of the SWCNT's cell was 2.4595 Å. The curve of potential energy versus step increase was shown in Fig. 2. Then, the Young's modulus can be calculated by the formula

$$Y = \frac{\Delta E}{A \cdot \Delta l} \cdot \frac{1}{\varepsilon}, \quad (9)$$

where  $\Delta E$  is the increment of the potential energy,  $A$  is the cross sectional area of SWCNT,  $\Delta l$  is the increment of the length, and  $\varepsilon = \Delta l/l_0$  is the strain of SWCNT. The Young's modulus of (3,3) SWCNT was  $1.4923 \pm 0.0263$  TPa.

MD simulations were performed in the canonical ensemble at a temperature of 0.01 K using the Nose–Hoover thermostat [25]. Since the target temperature  $T$  cannot be 0.0 K, which is not allowed in the Nose–Hoover formulation, here 0.01 K was used to

**Fig. 1.** The SWCNT model with triclinic cell and chirality (3,3) used in calculation.

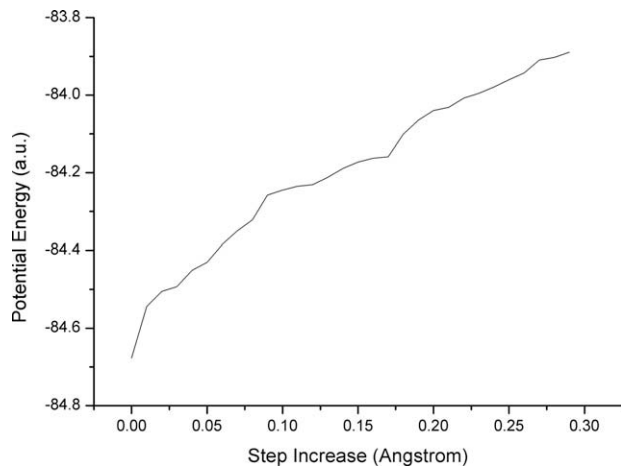


Fig. 2. Potential energy vs. step increase using CPMD method.

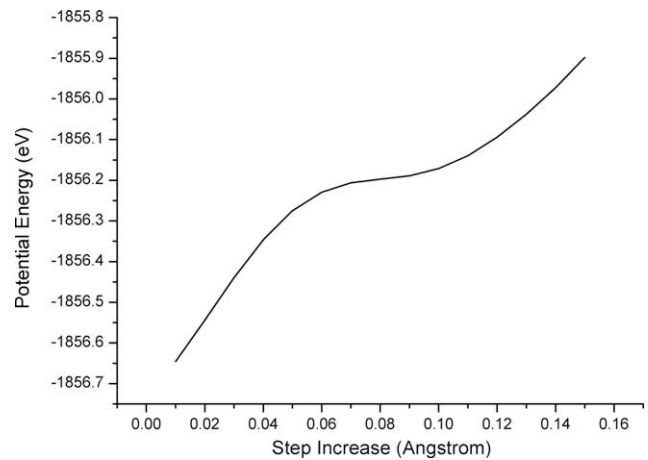


Fig. 4. Potential energy and step increase using DFT method.

achieve similar conditions as that in CPMD and DFT simulations. The equations of motion were integrated using the velocity-Verlet algorithm [26] with a timestep of 1 fs. The system was equilibrated for 50 ps before data collection. After the equilibrium, the SWCNT was stretched along the axis with one end fixed. The strain rate was  $2 \times 10^9 \text{ s}^{-1}$ , that is, 1.0% strain was imposed each time and then the SWCNT is dynamically relaxed for 5 ps to obtain the microscopic equilibrium configuration. During the simulation, the stress tensor of the SWCNT was calculated in the form

$$\sigma^{\alpha\beta} = \frac{1}{\Omega} \left[ - \sum_i m_i v_i^\alpha v_i^\beta + \frac{1}{2} \sum_i \sum_{j \neq i} F_{ij}^\alpha r_{ij}^\beta \right], \quad (10)$$

where the summation is over all the atoms occupying the total volume  $\Omega$ , the first term and the second term in the square brackets are a kinetic energy contribution for atom  $i$  and a potential one, respectively.  $m_i$  and  $v_i$  are the mass and velocity of atom  $i$ ,  $F_{ij}$  are the forces between atoms  $i$  and  $j$ , and the indices  $\alpha$  and  $\beta$  denote the Cartesian components.  $r_{ij}^\alpha$  are the projection of the inter-atomic distance vectors along coordinate  $\alpha$ .

The stress-strain relationship was shown in Fig. 3. The square dots in Fig. 3 denoted the value of the average stress along the stretching direction. The Young's modulus was obtained by linear fit to these data. The result was  $1.0819 \pm 0.0084 \text{ TPa}$ . The curve did not go through the origin because we used an initial configura-

tion without relaxation which would not affect the slope of the curve.

Similar to the CPMD simulation, DFT simulations computed the energy of static state of CNT. Fig. 4 depicted the CNT energy with respect to the step. The Eq. (9) was used to compute the Young's modulus and the modulus was  $2.1216 \pm 0.4536 \text{ TPa}$ , which is higher than the other two methods.

Among the three results, the DFT result is the highest one. The MD result is the lowest. We considered the approaches employed in potentials used in MD and the pseudopotentials used in CPMD affect the interactions between atoms. In the CPMD scheme, only the valence electrons were treated quantum-mechanically, while the atomic cores were considered as classical particles. The interactions between the valence electrons and the atomic cores were represented by the pseudopotentials. To a certain extent, these pseudopotentials would weaken the interactions between the cores of atoms and the electrons. As well the quality of the pseudopotentials which are necessary inputs for any *ab initio* simulations is an important issue for CPMD calculation. The empirical force fields used in MD simulation, taking some specific equations to describe the forces act on the atoms, are difficult to manifest the interactions in the atomic system fully. Therefore, the differences between the three results are comprehensive and reasonable.

Additionally, in the MD simulation, we utilized another force field named adaptive intermolecular reactive empirical bond order (AIREBO) which is similar to Qin's work [9] in simulating intramolecular junctions between different CNTs to parameter the SWCNT and the obtained moduli are approximately equal to Qin's results. This force field dependent phenomenon reveals that the force fields utilized in simulation would also affect the final result.

In the simulation process, we also compared the time consuming for the same system. We found that CPMD is more time consuming compared with MD but less than DFT. CPMD would be 30 times more time consuming than MD. We used a single CPU (2 cores, master frequency is 2.60 GHz), MD method used up 2 h in simulation, while for CPMD it was up to 3 days to finish the same task. Some researchers compared the time consuming between the CPMD and MD simulation in their works [27] also demonstrated similar results.

#### 4. Conclusion

In this work, we compared the Young's modulus of chirality (3,3) SWCNT calculated by three different methods: CPMD, MD and DFT, systematically. The results given by the methods are in accord with the experiments performed by Treacy [28] and Krish-

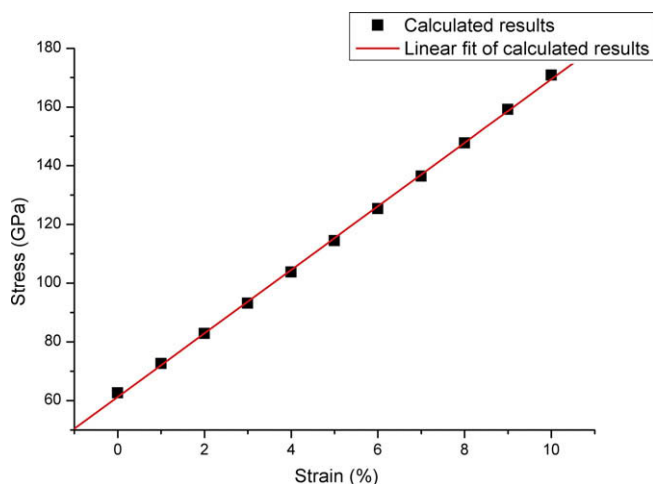


Fig. 3. Stress-strain relation of CNTs using MD method.

nan [29]. This work firstly compared three different methods which were adopted in nano-scale researches. CPMD, which is a typical *ab initio* MD, still has the difficulties in studying significantly larger systems. A novel *ab initio* MD method, suitable for simulating more atoms, is desirable. Classical MD allows calculations on systems containing significant numbers of atoms in a relatively long duration. However, current empirical potential functions are not accurate enough to reproduce the dynamics of molecular systems. DFT is expected to be applied in a larger system in the further. In conclusion, we hope that the present work would be helpful for sorting an appropriate method in simulating other nanomaterials.

## Acknowledgments

This work was jointly supported by the National High-tech R&D Program of China (863 Program, Grant Nos. 2007AA04Z348 and 2007AA021803), National Basic Research Program of China (973 Program, Grant No. 2007CB310500) and National Natural Science Foundation of China (NSFC, Grant Nos. 10772180 and 10721202).

## References

- [1] S. Iijima, Nature 354 (1991) 56–58.
- [2] M. Terrones, Ann. Rev. Mater. Res. 33 (2003) 419–501.
- [3] R.H. Baughman, A.A. Zakhidov, W.A. de Heer, Science 297 (2002) 787–792.
- [4] R.E. Smalley, M.S. Dresselhaus, G. Dresselhaus, P. Avouris, Carbon Nanotubes Synthesis, Structure, Properties and Applications, Springer, Berlin, 2001. pp. 391–425.
- [5] G. Overney, W. Zhong, D. Tomanek, Z. Phys. D 27 (1993) 93–96.
- [6] B.I. Yakobson, C.J. Brabec, J. Bernholc, Phys. Rev. Lett. 76 (1996) 2511–2514.
- [7] D.H. Robertson, D.W. Brenner, J.W. Mintmire, Phys. Rev. B 45 (1992) 12592–12595.
- [8] N. Yao, V. Lordi, J. Appl. Phys. 84 (1998) 1939–1943.
- [9] Z. Qin, Q.H. Qin, X.Q. Feng, Phys. Lett. A 372 (2008) 6661–6666.
- [10] R. Car, M. Parrinello, Phys. Rev. Lett. 55 (1985) 2471–2474.
- [11] A.R. Leach, Molecular Modelling: Principles and Applications, second ed., Pearson, England, 2001.
- [12] R.G. Parr, W. Yang, Density-Functional Theory of Atoms and Molecules, Oxford University Press, Oxford, 1989.
- [13] M.P. Allen, D.J. Tildesley, Computer Simulation of Liquids, Clarendon Press, Oxford, 1987.
- [14] D.C. Rapaport, The Art of Molecular Dynamics Simulation, second ed., Cambridge University Press, Cambridge, 2004.
- [15] S. Goedecker, M. Teter, J. Hutter, Phys. Rev. B 54 (1996) 1703–17010.
- [16] CPMD, <<http://www.cpmd.org/>>, Copyright IBM Corp 1990–2008, Copyright MPI für Festkörperforschung Stuttgart 1997–2001.
- [17] A.T. Hagler, E. Huler, S. Lifson, J. Am. Chem. Soc. 96 (1974) 5319–5327.
- [18] S.J. Plimpton, J. Comput. Phys. 117 (1995) 1–19.
- [19] M.D. Segall, P.J.D. Lindan, M.J. Probert, C.J. Pickard, P.J. Hasnip, S.J. Clark, M.C. Payne, J. Phys.: Condens. Matter 14 (2002) 2717–2744.
- [20] Y. Cho, C. Kim, H. Moon, Y. Choi, S. Park, C.K. Lee, S. Han, Nano Lett. 8 (2008) 81–86.
- [21] Z.H. Guo, X.H. Yan, Y.R. Yang, Y.X. Deng, D. Lu, D.L. Wang, J. Phys. Chem. 112 (2008) 4618–4621.
- [22] Z.X. Guo, J.W. Ding, Y. Xiao, D.Y. Xing, Nanotechnology 18 (2007) 465706–465711.
- [23] J.P. Perdrew, K. Burke, M. Ernzerhof, Phys. Rev. Lett. 77 (1996) 3865–3868.
- [24] H.J. Monkhorst, J.D. Pack, Phys. Rev. B 16 (1977) 1748–1749.
- [25] W.G. Hoover, Phys. Rev. A 31 (1985) 1695–1697.
- [26] L. Verlet, Phys. Rev. 159 (1967) 98–103.
- [27] M. Hawlitzky, J. Horbach, S. Ispas, M. Krack, K. Binder, J. Phys.: Condens. Matter 20 (2008) 285106–285120.
- [28] M.M.J. Treacy, T.W. Ebbesen, J.M. Gibson, Nature 381 (1996) 678–680.
- [29] A. Krishnan, E. Dujardin, T.W. Ebbesen, Phys. Rev. B 58 (1998) 14013–14019.